Single Molecule Tribology: Force Microscopy Manipulation of a Porphyrin Derivative on a Copper Surface

Supplementary Materials

R´emy Pawlak,[*,†] Wengen Ouyang,[‡] Alexander E. Filippov,[§] Lena Kalikhman-Razvozov,[‖] Shigeki Kawai,[†] Thilo Glatzel,[†] Enrico Gnecco,[¶] Alexis Baratoff,[†] Quanshui Zheng,[‡] Oded Hod,[‖] Michael Urbakh,[*,‖] and Ernst Meyer[*,†]

[†] *Department of Physics, University of Basel, Klingelbergstrasse 82, Basel 4056, Switzerland*

[‡] *Center for Nano and Micro Mechanics, Tsinghua University, Beijing 100084, China*

[§] *Donetsk Institute for Physics and Engineering, National Academy of Sciences of Ukraine, Donetsk 83114, Ukraine*

[‖] *Department of Physical Chemistry, School of Chemistry, The Raymond and Beverly Sackler Faculty of Exact Sciences and The Sackler Center for Computational Molecular and Materials Science, Tel Aviv University, Tel Aviv 6997801, Israel*

[¶] *Otto Schott Institute of Materials Research (OSIM), Friedrich Schiller University Jena, Jena 07743, Germany*

E-mail: remy.pawlak@unibas.ch; urbakh@post.tau.ac; ernst.meyer@unibas.ch

Theory and computation

Parameterization via density functional theory calculations

The extended Prandtl-Tomlinson model requires as input several spring constants. These where obtained via density functional theory calculations (DFT). In Fig. S1 we schematically present the decorated porpyrin molecule and indicate the various degrees of freedom considered in the simulations. Fig. S2 presents the energy variations for stretching, bending, and rotation of the bond connecting the connecting the di-cyanophenyl side group as obtained using the B3LYP exchange-correlation density functional approximation and the 6-31G** atom-centered basis set. Using simple least-square parabolic fits to the calculated data the corresponding spring constants have been extracted. In Fig. S3 similar results are presented for the bond between the CN end-group and the di-cyanophenyl ring. Basis set convergence tests shown in Fig. S3 indicate that the 6-31G** basis set results are satisfactory.

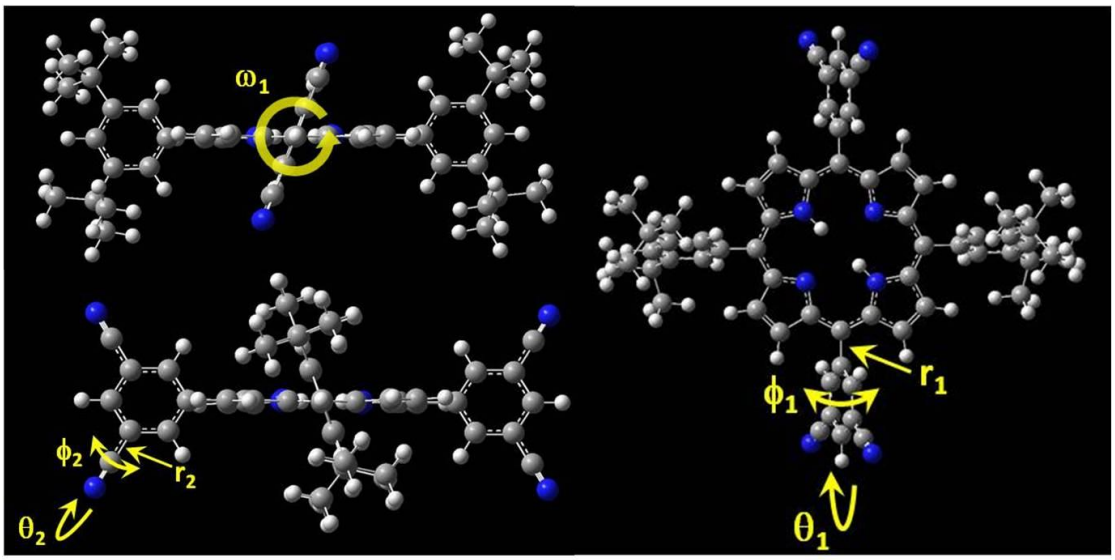

Figure S1: Schematic presentation of the decorated porphyrin molecule and definition of the degrees of freedom considered in the density functional theory calculations.

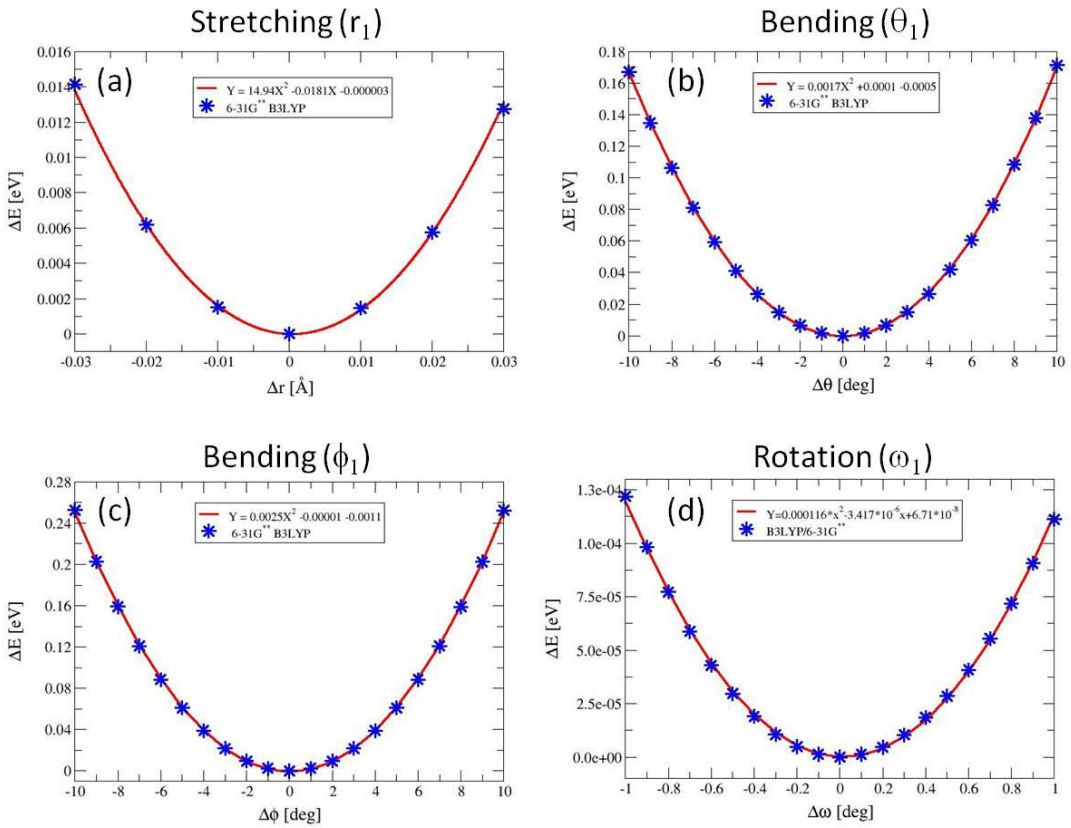

Figure S2: Energy as a function of (a) stretching and compression; (b),(c) bending along the θ and ϕ angles, respectively; and (d) rotation around the axis of the bond connecting the di-cyanophenyl side group and the porphyrin backbone. Calculated data obtained at the B3LYP/6-31G** level of theory is designated by blue stars and parabolic fits appear as red lines.

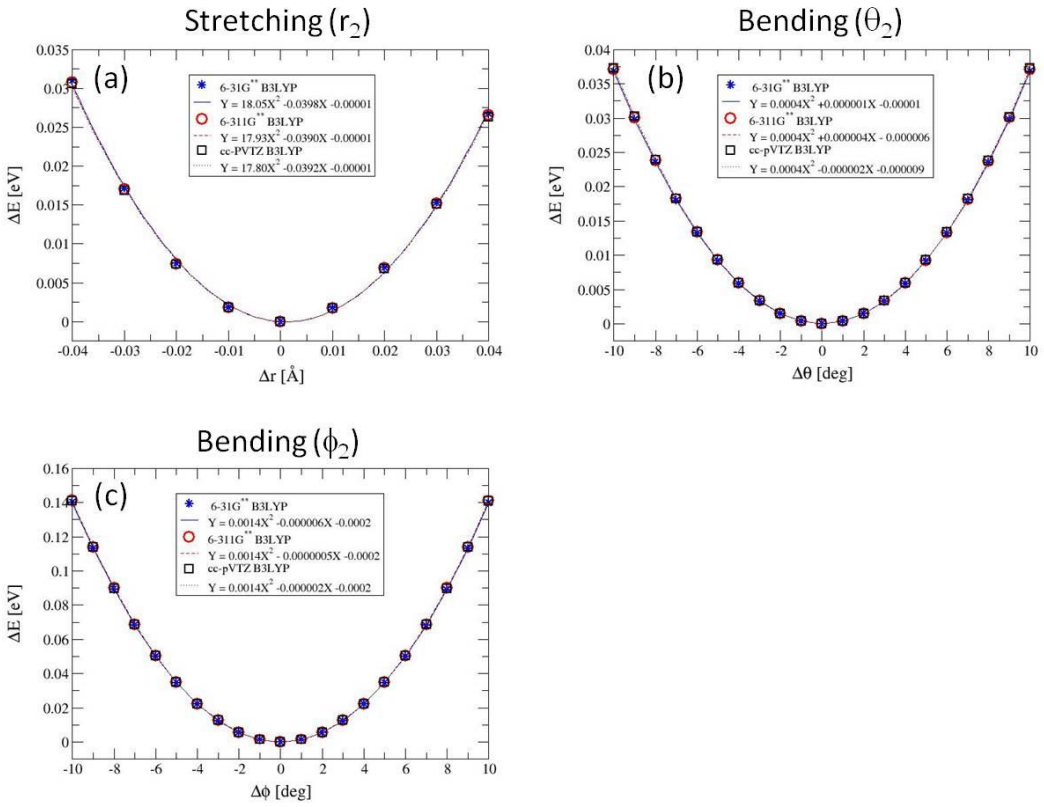

Figure S3: Energy as a function of (a) stretching and compression and (b),(c) bending along the θ and ϕ angles, respectively of the bond between the CN end-group and the di-cyanophenyl ring. Calculated data obtained using the B3LYP exchange-correlation density functional approximation and the 6-31G**, 6-311G**, and cc-pVTZ basis sets is designated by symbols and parabolic fits appear as lines.

Deriving the effective stiffness from DFT results

In our extended Prandtl-Tomlinson model we define a single effective spring (see Fig. S4) that takes into account the stiffnesses $\boldsymbol{K}_1 = \left(K_{r_1}, K_{\theta_1}, K_{\phi_1}, K_{\omega_1}\right)$, $\boldsymbol{K}_2 = \left(K_{r_2}, K_{\theta_2}, K_{\phi_2}\right)$ and equilibrium bond lengths r_1^0 and r_2^0 provided by the DFT calculation. Here, K_{r_i} with i=1,2 is the bond stretching stiffness, $K_{\phi 1}, K_{\theta_2}$ and $K_{\theta 1}, K_{\phi_2}$ are the stiffness corresponding to out-of-plane (the phenyl plane) bending and in-plane bending of bond, respectively and K_{ω_1} is the torsional stiffness of bond 1 (see Fig. S1). The effective spring is characterized by a single stiffness vector $\boldsymbol{K} = \left(K_{r'}, K_{\theta'}, K_{\phi'}\right)$ and equilibrium distance r_0' represented in the local coordinate system of the molecule (see Fig. 5 of the main text). We note that the parameters of the effective spring do not depend on the equilibrium angles but rather on angle variations.

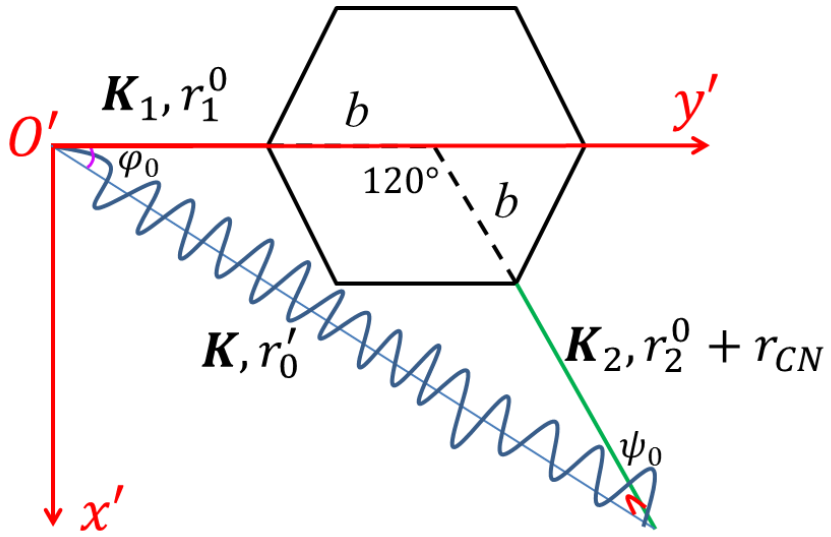

Figure S4. Schematics of the effective spring model definition.

The relations between $\boldsymbol{K}$, $\boldsymbol{K}_1$, and $\boldsymbol{K}_2$ can be found by applying perturbative stretching and rotation to the considered degrees of freedom leaving the leading terms. The resulting relations are as follows:

$$\frac{1}{K_{r'}} = \frac{\cos^2\varphi_0}{K_{r_1}} + \frac{\cos^2\psi_0}{K_{r_2}} + \frac{(r_{10}+b)(r_{20}+r_{CN})^2}{r_0'}\frac{\sin 2\pi/3 \cdot \sin\psi_0}{K_{\phi 2}}$$

$$\frac{1}{K_{\theta'}} = \frac{\cos^2\varphi_0}{K_{\phi_1}} + \frac{r_2^0 + r_{CN}}{r_0'}\left(\frac{2}{K_{\phi_1}} + \frac{\cos\psi_0}{K_{\theta_2}}\right) + \frac{\sin^2\varphi_0}{K_{\omega_1}}$$

$$\frac{1}{K_{\phi'}} = \frac{1}{K_{\theta_1}}\left[1 + \left(\frac{r_2^0 + r_{CN}}{r_0'}\frac{K_{\theta 1}}{K_{\phi_2}}\right)^2 + 2\frac{r_2^0 + r_{CN}}{r_0'}\frac{K_{\theta 1}}{K_{\phi_2}}\cos\psi_0\right]^{\frac{1}{2}}$$

where,

$$r_0' = \sqrt{(r_1^0 + b)^2 + (r_2^0 + r_{CN} + b)^2 - 2(r_1^0 + b)(r_2^0 + r_{CN} + b)\cos(2\pi/3)}$$

$$r_0'\cos\varphi_0 = (r_1^0 + b) - (r_2^0 + r_{CN} + b)\cos(2\pi/3)$$

$$r_0'\cos\psi_0 = (r_2^0 + r_{CN} + b) - (r_1^0 + b)\cos(2\pi/3)$$

$b = 1.405$ Å is the carbon-carbon bond length of the benzene ring, and $r_{CN} = 1.136$ Å is the carbon-nitrogen bond length of the CN group. As stated above, by using the above relations the stiffnesses and equilibrium distance of the effective spring can be extracted from the DFT results. The DFT input values are detailed in Tab. S1 and the effective spring parameter values are listed in Tab. I of the main text.

K_{r_1}	29.84 eV/Å^2	K_{r_2}	36.10 eV/Å^2
K_{θ_1}	3.4 meV/$^{\circ 2}$	K_{θ_2}	0.8 meV/$^{\circ 2}$
K_{ϕ_1}	5.0 meV/$^{\circ 2}$	K_{ϕ_2}	2.8 meV/$^{\circ 2}$
K_{ω_1}	0.233 meV/$^{\circ 2}$	----	----
r_1^0	1.498 Å	r_2^0	1.435 Å

Table S1: Parameter values extracted from the DFT calculations.

Dynamic equations

Due to its large mass the dynamics of the driven tip is given by Newton's equations of motion whereas for the effective spring representing the molecule we apply the Langevin equations as follows:

$$\begin{cases} M\ddot{X}(t)+\Gamma_X\dot{X}+\gamma_{mt}(\dot{X}-\dot{x})+K_{xx}(x-X-l_x)+K_{xy}(y-Y-l_y)+K_{xz}(z-Z-l_z)+k_X\left[X-X_0^{DR}-V_X(t-t_0)\right]=0 \\ M\ddot{Y}(t)+\Gamma_Y\dot{Y}+\gamma_{mt}(\dot{Y}-\dot{y})+K_{yx}(x-X-l_x)+K_{yy}(y-Y-l_y)+K_{yz}(z-Z-l_z)+k_Y\left[Y-Y_0^{DR}-V_Y(t-t_0)\right]=0 \\ M\ddot{Z}(t)+\Gamma_Z\dot{Z}+\gamma_{mt}(\dot{Z}-\dot{z})+K_{zx}(x-X-l_x)+K_{zy}(y-Y-l_y)+K_{zz}(z-Z-l_z)+k_Z\left[Z-Z_0^{DR}-V_Z(t-t_0)\right]=0 \\ \gamma_{ms}\dot{x}+\gamma_{mt}(\dot{x}-\dot{X})+K_{xx}(x-X-l_x)+K_{xy}(y-Y-l_y)+K_{xz}(z-Z-l_z)+\dfrac{\partial U_{ms}}{\partial x}=f_x \\ \gamma_{ms}\dot{y}+\gamma_{mt}(\dot{y}-\dot{Y})+K_{yx}(x-X-l_x)+K_{yy}(y-Y-l_y)+K_{yz}(z-Z-l_z)+\dfrac{\partial U_{ms}}{\partial y}=f_y \\ \gamma_{ms}\dot{z}+\gamma_{mt}(\dot{z}-\dot{Z})+K_{zx}(x-X-l_x)+K_{zy}(y-Y-l_y)+K_{zz}(z-Z-l_z)+\dfrac{\partial U_{ms}}{\partial z}=f_z \end{cases}$$

The first three equations describe the motion of the tip (with mass *M*), and the rest ones correspond to the molecule motion (overdamped equations). U_{ms} describes the interaction between the end group of the molecule and the Cu(111) surface (see equations 1-3 in the main text), and (f_x, f_y, f_z) are the random forces experienced by the molecule in the *x*, *y*, and *z* directions. The parameters $\Gamma_i = 2\sqrt{k_i M}, i = X, Y, Z$ describe the dissipation of the kinetic energy of the tip in *X*, *Y*, and *Z* directions, and γ_{ms} and γ_{mt} are responsible for the energy dissipation at the molecule-substrate and molecule-tip interfaces, respectively. The random forces (f_x, f_y, f_z) and the damping coefficients γ_{ms} and γ_{mt} obey the fluctuation-dissipation theorem. The values $(X_0^{DR}, Y_0^{DR}, Z_0^{DR})$ define the position of the stage, and the lengths (l_x, l_y, l_z) are the

equilibrium lengths of the effective spring characterizing the molecule. The vector (k_X, k_Y, k_Z) defines the cantilever stiffness and the matrix $[K]_{ij}, i, j = x, y, z$ is the matrix of stiffnesses of the molecule spring in the Cartesian coordinates which can be calculated using the following transformation:

$$[K] = [T] \begin{pmatrix} K_{r'} & 0 & 0 \\ 0 & K_{\theta'}/r'^2 & 0 \\ 0 & 0 & K_{\phi'}/r'^2 \sin^2\theta' \end{pmatrix} [T]^{-1}$$

where

$$[T] = \begin{pmatrix} \cos\beta & \cos\alpha\sin\beta & \sin\alpha\sin\beta \\ -\sin\beta & \cos\alpha\cos\beta & \sin\alpha\cos\beta \\ 0 & -\sin\alpha & \cos\alpha \end{pmatrix} \begin{pmatrix} \sin\theta'\cos\phi' & \cos\theta'\cos\phi' & -\sin\phi' \\ \sin\theta'\sin\phi' & \cos\theta'\sin\phi' & \cos\phi' \\ \cos\theta' & -\sin\theta' & 0 \end{pmatrix}.$$

Here, α and β are the orientation angles of the molecular plane with respect to the copper surface as illustrated in Fig.5 of the main text. In order to reduce the parameter space we choose the Euler angle $\psi = 0^\circ$ (angle of rotation around the z' axis), thus ignoring different yawning positions of the molecule with respect to the tip. With this choice the angles α and β coincide with the Euler angles θ (angle of rotation around the x' axis) and ϕ (angle of rotation around the z axis), respectively.

Similarity, the equilibrium lengths of the effective spring (l_x, l_y, l_z) can be written as

$$\begin{pmatrix} l_x \\ l_y \\ l_z \end{pmatrix} = \begin{pmatrix} \cos\beta & \cos\alpha \cdot \sin\beta & \sin\alpha \cdot \sin\beta \\ -\sin\beta & \cos\alpha \cdot \cos\beta & \sin\alpha \cdot \cos\beta \\ 0 & -\sin\alpha & \cos\alpha \end{pmatrix} \begin{pmatrix} r'_0 \sin\theta'_0 \cos\phi'_0 \\ r'_0 \sin\theta'_0 \sin\phi'_0 \\ r'_0 \cos\theta'_0 \end{pmatrix}$$

M	k_X	k_Y	k_Z	V_{dr}	V_{app}	γ_{ms}	γ_{mt}
10^{-12} kg	6 N/m	6 N/m	60 N/m	25 nm/s	10 nm/s	10^{-7} kg/s	10^{-7} kg/s

Table S2: Parameter values used in the dynamic simulations. Here, V_{dr} and V_{app} are the pulling velocities used in the simulations of friction and approach-retraction, respectively.